Remote Sens. **2014**, *6*, 12217-12233; doi:10.3390/rs61212217

OPEN ACCESS

remote sensing

ISSN 2072-4292

www.mdpi.com/journal/remotesensing

Article

Error Analysis on ESA's Envisat ASAR Wave Mode Significant Wave Height Retrievals Using Triple Collocation Model

He Wang [1,2,3,*,†], Jianhua Zhu [1] and Jingsong Yang [2]

[1] National Ocean Technology Center, State Oceanic Administration, Tianjin 300112, China; E-Mail: besmile@263.net

[2] State Key Laboratory of Satellite Ocean Environment Dynamics, Second Institute of Oceanography, State Oceanic Administration, Hangzhou 310012, China; E-Mail: jsyang@sio.org.cn

[3] Laboratoire d'Océanographie Spatiale, Institut Français de Recherche pour l'Exploitation de la Mer, Brest 29280, France

† This paper was first presented in the 35th International Symposium on Remote Sensing of Environment. Wang, H.; Shi, C.-Y.; Zhu, J.-H.; Huang, X.-Q.; Chen, C.-T. Validation of significant wave height product from Envisat ASAR using triple collocation. *IOP Conf. Ser.: Earth Environ. Sci.* **2014**, *17*, doi:10.1088/1755-1315/17/1/012279.

* Author to whom correspondence should be addressed; E-Mail: wanghe08@gmail.com; Tel.: +86-22-2753-6515; Fax: +86-22-2736-7824.

External Editors: James Churnside and Prasad S. Thenkabail

Received: 18 July 2014; in revised form: 20 November 2014 / Accepted: 28 November 2014 / Published: 8 December 2014

Abstract: Nowadays, spaceborne Synthetic Aperture Radar (SAR) has become a powerful tool for providing significant wave height (SWH). Traditionally, validation of SAR derived SWH has been carried out against buoy measurements or model outputs, which only yield an inter-comparison, but not an "absolute" validation. In this study, the triple collocation error model has been introduced in the validation of Envisat ASAR derived SWH products. SWH retrievals from ASAR wave mode using ESA's algorithm are validated against *in situ* buoy data, and wave model hindcast results from WaveWatch III wave model, covering a period of six years. From the triple collocation validation analysis, the impacts of the collocation distance and water depth on the error of ASAR SWH are discussed. It is found that the error of Envisat ASAR SWH product is linear to the collocation distance, and decrease with the decreasing collocation distance. Using the linear regression fit method, the

absolute error of Envisat ASAR SWH was obtained with zero collocation distance. The absolute Envisat ASAR wave height error of 0.49 m is presented in deep and open ocean from this triple collocation validation work, in contrast to a larger error of 0.56 m in coastal and shallow waters. One of the reasons for the larger Envisat ASAR SWH errors in the coastal waters may be the inaccurate Modulation Transfer Function (MTF) adopted in the Envisat ASAR wave retrieval algorithm.

Keywords: Envisat ASAR; significant wave height; validation; triple collocation

1. Introduction

Significant wave height (SWH) of ocean surface wave is one of the most important parameters for offshore engineering application and ocean model forecast. Since decades ago, the spaceborne Synthetic Aperture Radar (SAR) has become a useful dataset for providing SWH, due to its high spatial resolution, wide spatial coverage and all-weather capability [1,2]. Especially, the SAR wave mode, which was employed by the European Remote Sensing Satellite-1/2 (ERS) SAR [3], Environmental Satellite (Envisat) Advanced Synthetic Aperture Radar (ASAR) [4–6], and is also adopted by the recently launched Sentinel-1A [7,8], could provide global coverage of ocean wave information since 1991. Since then, the SAR wave mode SWH data have been used in the various applications from the ocean wave assimilation [9] to swell dissipation estimation [10] or swell source identification [11]. However, the error analysis and quality assessment on these datasets are of vital importance to meet the requirement of these applications.

Numerous studies have been carried out for the validation of SAR derived SWH data. Traditionally, the validations were performed against the buoy measurements (e.g., [12–17]) or the ocean wave model outputs (e.g., [18,19]). In such type of validation works, the quality of the SAR SWH products was simply assessed through the direct comparison using the standard statistical methods (e.g., estimation of bias and/or Root Mean Square Error), assuming no error in the buoy observations or ocean wave model output results. However, this assumption does not hold strictly as both buoy and model data are subject to errors. On one hand, besides the instrument error of buoys, the sampling variability may not be negligible owing to the noticeable collocation distance of the observations from the buoy and the satellite [20]. On the other hand, the quality of ocean wave model results is limited by the model configuration, parameterization and the input wind forcing. Thus, not only the error of SAR retrievals but also other factors may contribute to the validation statistics. Therefore, these methods only yield an inter-comparison, but not an "absolute" validation.

In contrast to those direct inter-comparisons, the triple collocation error model, in which the errors in all the collocated triple datasets are taken into account, has been proposed [21]. The novel and advanced error model requires three datasets, including *in situ*, remote sensed and model data, with an independent error structure. And this contributes to its major advantage of simultaneously providing the error statistics in each product and the relationships between different datasets. Therefore, this technique could significantly improve the traditional scheme of validation, calibration, and bias correction for geophysical variables. This methodology is now widely used in the validations of remote sensed data in oceanography research field, such as the ocean wind and stress (e.g., [22–24]). Although some researchers have applied the triple

collocation error model to carry out the error estimation and analysis for the wave height derived from the altimeters of ERS-2, Jason-1/2, and Envisat (e.g., [25–27]), this powerful method of error analysis has not been employed in the validation of significant wave height retrievals from SAR data until now.

Moreover, the optimal choice of collocation distance (or space window) is very often a puzzling challenge in the calibration and/or validation work for wind or wave data [28,29]. In practice, this problem could be more severe for the case of SAR wave mode observations than altimeter data. Because SAR data density is smaller (an average of 100 km between data points for the Envisat ASAR wave mode), and the numbers of buoys with open access data are too limited, the SAR wave mode measurements and the buoys have very little opportunity to be collocated exactly in space. Therefore, the collocation distance between SAR and buoy is an important issue in the validation work, not only for the triple collocation, but also for the inter-comparison against buoy.

In this paper, for the first time, the triple collocation error model is introduced in the validation of Envisat ASAR wave mode SWH data, in order to estimate the "absolute" error of ASAR derived SWH, and compare its quality to the datasets from buoys and wave model hindcast. The impact of the collocation distance and water depth on the error of ASAR wave height is also discussed.

2. Data Description

2.1. Envisat ASAR Wave Mode Data

The SAR acquisition mode, so-called wave mode, is dedicated to detect the ocean wave information on global basis. In this wave mode, the Envisat ASAR has generated huge number of small SAR images (called imagettes) of 7 by 10 km every 100 km at the incidence angle of 23° and VV polarization, from its launch in March 2002 to the end of the mission in April 2012. The Envisat ASAR wave mode data used here were taken from 2003 to 2008, covering a period of six years. Examples of these Envisat ASAR imagette are shown in Figure 1.

Under the quasi-linear assumption of SAR-Ocean imaging mechanism, European Space Agency (ESA) used a methodology to produce a level 2 wave mode product of ocean wave spectrum without a priori information [30,31]. The cross spectra technique [32] was also employed in the inversion scheme to remove the 180° ambiguity in wave propagation direction. From the inverted ocean wave spectra the significant wave height H_s could be obtained by

$$H_s = 4\sqrt{\int d\alpha \int df F(f,\alpha)} \tag{1}$$

where $F(f, \alpha)$ represents the wave spectra in frequency (f) and direction (α) space.

Although the level 2 ASAR products contain the ocean wave spectra, the objective of this paper is only limited to the quality assessment of the SWH product. The major reason for the limit is that the number of directional wave buoys deployed in the ocean is too small to achieve a triple collocated dataset of wave spectra as large as that of SWH. As discussed in the Section 4.1, the triple collocation analysis requires a large dataset to produce the reliable results, and the SWH, but not wave spectra, could meet the requirement.

Figure 1. Envisat ASAR imagette acquired on (**a**) 01 August 2008 20:49:43; (**b**) 1 January 2007 01:52:24; and (**c**) 30 October 2008 22:08:29; with the image variance of 2.34, 1.02 and 1.30, respectively.

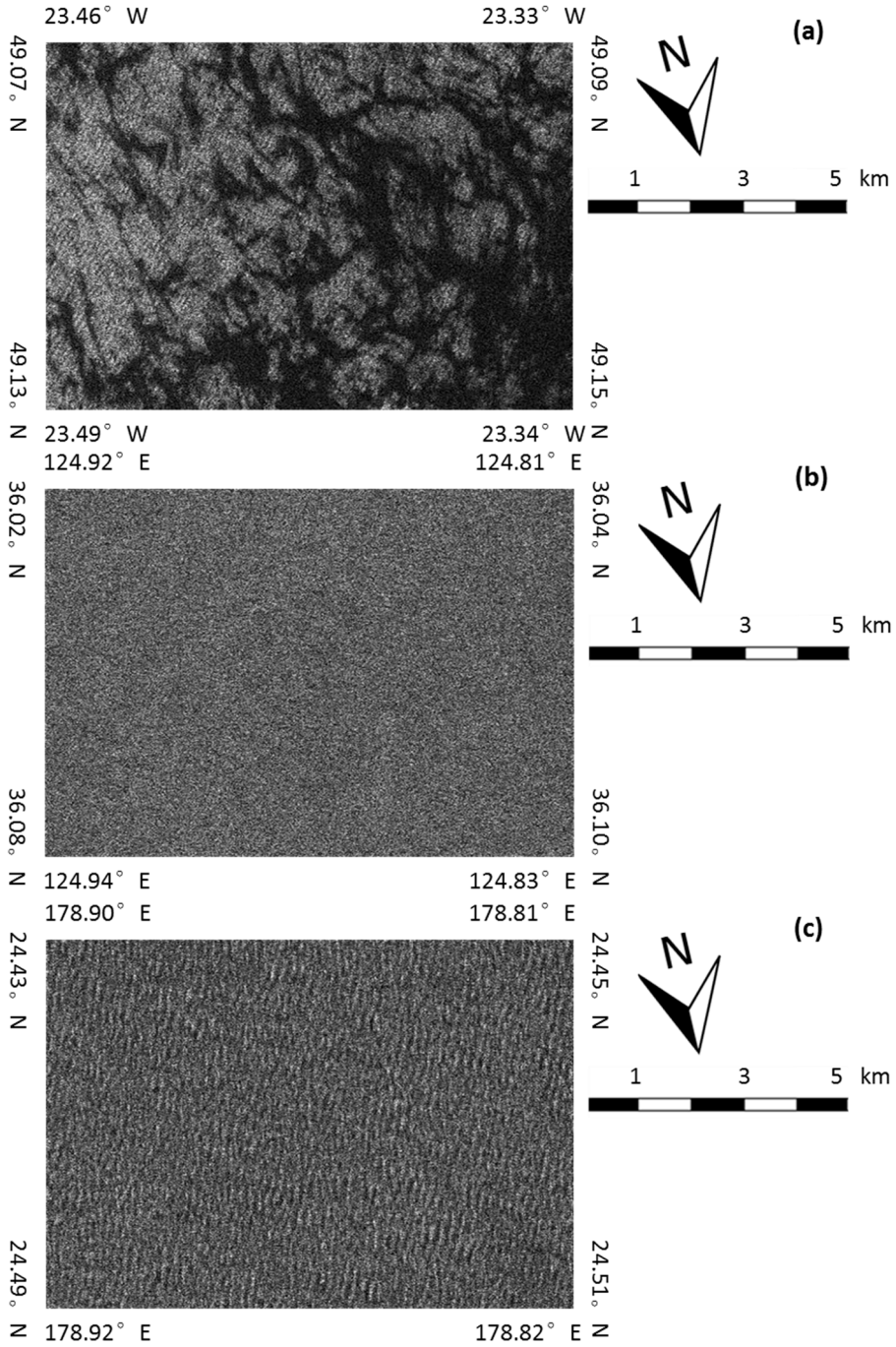

The data used in the validation were selected by a quality control procedure. After been filtered using fields of "land_flag" and "quality_flag" from the Envisat ASAR wave mode product files, inhomogeneous or noisy imagettes were identified and excluded if their image variance greater than 1.4 or smaller than 1.05. The parameter image variance is defined as the imagette variance normalized with mean imagette intensity. This homogeneity quality control check was carried out in order to filter out the non-wave features, such as oil slicks, sea ice, or atmospheric boundary roll, *etc.*, which may influence the ESA's ocean wave spectra retrieval scheme and the SWH data. Take the three Envisat ASAR imagettes shown in

Figure 1 for example. SAR imagettes in Figure 1a,b are inhomogeneous and noisy to detect wave-like pattern, respectively. Only the SAR imagettes with image variance from 1.05 to 1.4, resulting in a rejection rate of 6.5%, such as Figure 1c could be passed the quality control and be used in the triple collocation.

2.2. Buoy Data

Significant wave height data have been collected from 152 buoys, which are freely available from National Oceanic and Atmospheric Administration's (NOAA) National Data Buoy Centre (NDBC). The buoy data used here are obtained from three buoy networks: NDBC, the Coastal Data Information Program (CDIP), and the Environment Canada's Marine Environmental Data Service (MEDS). The locations of the buoys used for this study are depicted in Figure 2.

Furthermore, the buoys deployed at deeper than 200 m water depth and greater than 50 km offshore distance, were selected, and with their locations shown in Figure 2 as red dots. The objective of subtracting these deep and open ocean buoys is to investigate the error characteristic in different water depth regions separately (See Subsection 4.3).

Figure 2. Locations of the 152 collocated buoys used in the validation. 54 of the buoys, deployed in the deep and open ocean are represented by red dots.

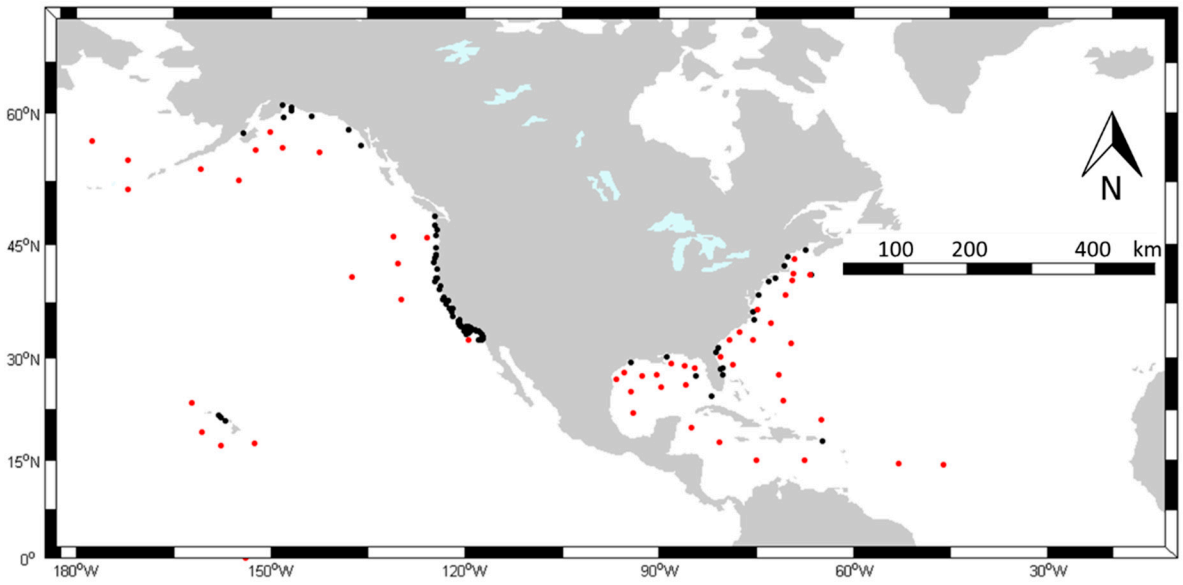

2.3. Wavewatch III SWH Hindcast

The third dataset used in this work are the significant wave height hindcast results from the database of IOWAGA (Integrated Ocean Waves for Geophysical and other Applications) project of IFREMER [33]. The wave hindcasts were performed using the ocean wave model of WaveWatch III (hereafter ww3), forced by the Climate Forecast System Reanalysis winds, on 0.5° × 0.5° global grid. The model uses a parameterization called TEST451, with significant improvements for swell dissipation [34,35]. The hindcast database also provides SWH outputs at the location of NDBC buoys, which are used in this work. All the ww3 model SWH hindcast data from IOWAGA used here could be freely available from IFREMER.

It should be noted here that, the IFREMER IOWAGA ww3 ocean wave hindcasts have not been assimilated with any observations (SAR or buoy) by now. Therefore, in the triple collocation datasets, the SWH data from Envisat ASAR, buoy, and model hindcast have independent errors. In this context, the errors of these independent triplets can be analyzed by the triple collocation error model, presented in the next section.

3. Triple Collocation Error Model

The triple collocation error model assumes that three SWH estimates H_{buoy} (from NDBC buoy observation), H_{ASAR} (from Envisat ASAR wave mode product) and H_{ww3} (from ww3 wave model hindcast), with their independent random errors (e_{buoy}, e_{ASAR} and e_{ww3}), are related to the hypothetical true significant wave height H linearly as shown below:

$$\begin{aligned} H_{buoy} &= \beta_{buoy} H + e_{buoy} \\ H_{ASAR} &= \beta_{ASAR} H + e_{ASAR} \\ H_{ww3} &= \beta_{ww3} H + e_{ww3} \end{aligned} \tag{2}$$

The linear calibration constants β_{buoy}, β_{ASAR} and β_{ww3} in Equation (2) can be eliminated by introducing new variables $H'_X = H_X/\beta_X$, $e'_{X'} = e_X/\beta_X$ (with subscript X standing for buoy, ASAR, and ww3, respectively), and then eliminate the unknown truth H utilizing the assumption of independent errors in order to obtain

$$\begin{aligned} \left\langle e_{buoy'}{}^2 \right\rangle &= \left\langle \left(H_{buoy}{}' - H_{ASAR}{}' \right)\left(H_{buoy}{}' - H_{ww3}{}' \right) \right\rangle \\ \left\langle e_{ASAR'}{}^2 \right\rangle &= \left\langle \left(H_{ASAR}{}' - H_{buoy}{}' \right)\left(H_{ASAR}{}' - H_{ww3}{}' \right) \right\rangle \\ \left\langle e_{ww3'}{}^2 \right\rangle &= \left\langle \left(H_{ww3}{}' - H_{buoy}{}' \right)\left(H_{ww3}{}' - H_{ASAR}{}' \right) \right\rangle \end{aligned} \tag{3}$$

The implementation of the triple collocation error model using the iteration procedure [26] can be outlined as follows. The procedure starts with the initial guess of $\beta_{ASAR} = 1$, $\beta_{ww3} = 1$ and scales H_{ASAR} and H_{ww3} with β_{ASAR} and β_{ww3}. In addition, first estimates for the errors and the calibration constants are determined using Equation (3) and a neutral regression [36], respectively. In the next step, H_{ASAR} and H_{ww3} are scaled with the newly found estimates for β_{ASAR} and β_{ww3}, and then the errors and the calibration constants are determined again, until the convergence is achieved.

The result of applying the above model is independent of which variables are chosen to be reference, thanks to is its symmetric nature. However, one reference has to be chosen, which means that only a relative calibration is possible [25,26]. In this work, buoy observations were chosen as the reference standard (β_{buoy}) and the calibration coefficients of β_{ASAR} and β_{ww3} were calculated.

Based on the triple collocation error model above, the statistics of the Root Mean Square Error (RMSE) and Scatter Index (SI) can be obtained for every individual data. The definitions are as follows:

$$RMSE_i = \sqrt{\left\langle e_i^2 \right\rangle} \tag{4}$$

$$SI_i = \frac{\sqrt{\left\langle e_i^2 \right\rangle}}{\left\langle H_i \right\rangle} \tag{5}$$

where the *i* subscript represents for buoy, ASAR, and ww3, respectively. The scatter index is a statistical metric for ocean wave data inter-comparison. Essentially, it is a normalized measure of error that takes into account the average of the wave data. Lower values of the SI are an indication of a better data quality.

4. Triple Collocation and Error Analysis

4.1. Collocation Criteria and Collocated Results

For validation purpose, the data from Envisat ASAR wave mode, buoy, and ww3 wave model should be triple collocated in time and space. The temporal interval was limited to less than 30 min for the triple datasets. For spatial collocation, only the distances between SAR and buoy have to be taken into consideration, because the ww3 hindcast model used here outputs SWH at the exact location of buoys.

Different distances between SAR imagettes and buoy observations have been chosen as maximum distance of collocation criteria, from 200 km to 10 km, stepped by 10 km. Figure 3 shows how this collocation procedure works as an example of 50 km. As shown in Figure 3, the distance between imagette acquired at 19:16 UTC on 10 January 2008 and the buoy in the west of Moresby Island (with NDBC buoy ID 46208) is 31 km, less than the chosen maximum collocation distance of 50 km presented in red dashed circle.

Figure 3. Collocation example of Envisat ASAR and NDBC buoy when the maximum collocation distance is set to be 50 km.

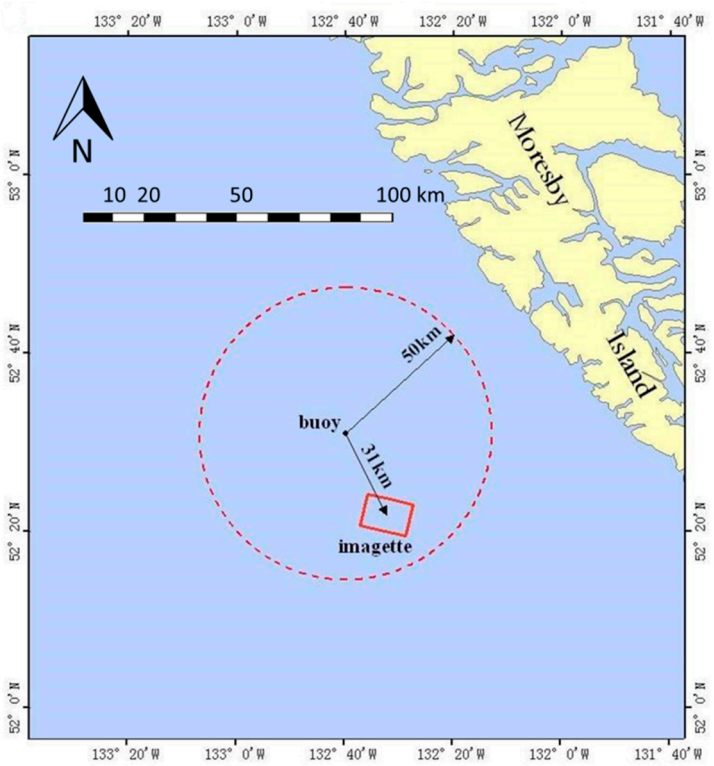

The numbers of triple collocated data points through different distances are shown in Figure 4. One can see that, the collocated numbers drop significantly with the decreasing collocation distance, both for all buoys and deep open ocean buoys. Even for all the buoys, only less than 100 data points could be found with 10 km collocated distance for six years, although the number is above 17,000 with 200 km distance.

Simulations indicated that more than 500 samples of collocated triplets are needed to achieve reliable results with small enough uncertainty [37]. In this work, we used a stricter standard of 1500 samples, which yields an uncertainty within 6% according to the study in [37]. Thus, the collocation datasets with collocation distance less than 50 km were excluded in the error analysis of following subsections.

Figure 4. Histograms of triple collocation numbers with the all buoys (**left**), and those in the deep and open ocean (**right**). The red lines represent the collocation numbers of 1500.

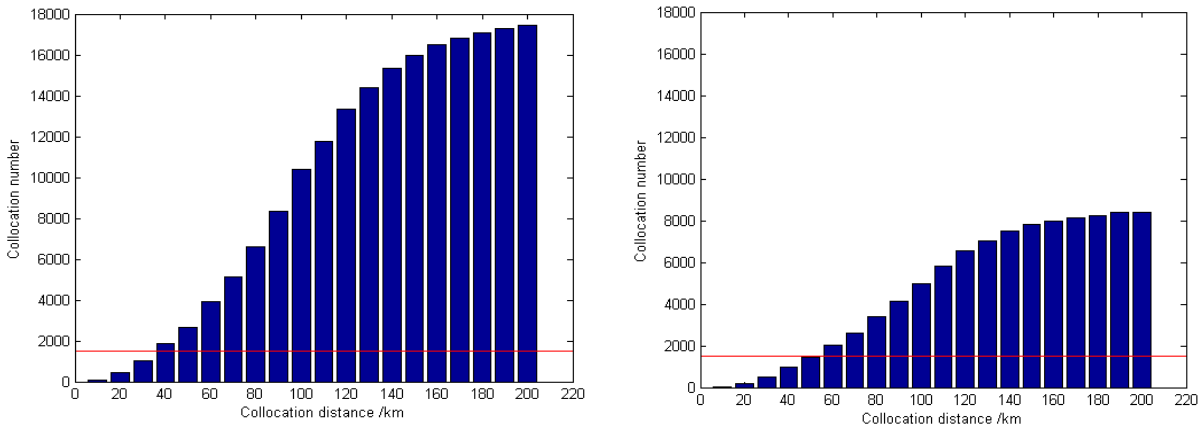

4.2. Triple Collocation Comparison Results

Using the triple collocation error model presented above, the significant wave height errors for each of the triple collocated datasets have been estimated. Figures 5 and 6 illustrate triple collocation comparison results of Envisat ASAR, NDBC buoy and ww3 wave model significant wave height data, with collocated distances of 50 km, 100 km, 150 km and 200 km, for collocations with all buoys and the deep and open ocean buoys, respectively. In order to look further into the trend of the comparison results, the estimates of calibrated coefficients, RMSE, and SI, for all collocated distances, are listed together in Tables 1 and 2. From Figures 5 and 6, one may be curious about the "empty" bins in the scatter plots with regard to NDBC buoy. In fact, this is because that the buoy SWH measurements have a resolution of 0.1 m, same as the histogram bin in the scatter plots, which is much lower than that of Envisat ASAR and ww3 SWH data.

Generally, both in terms of RMSE and SI, the significant wave height errors from Envisat ASAR are found to be the largest, followed by the buoy SWH measurements errors, while the ww3 wave model hindcasts have the best performance. The SWH errors of buoy and ww3 wave model are comparable, as their RMSE and SI have the order of 0.2 m and 10%, respectively. However, the SWH error of Envisat ASAR wave mode is much larger, with the order of 0.5 m and 24% for RMSE and SI.

It is clear that errors of buoy and ASAR SWH increase by increasing the collocation distance, both in terms of RMSE and SI, irrespective of the location of buoys. However, the variation of ww3 wave model errors with respect to the collocation distance does not show the apparent linear tendency as ASAR and buoy. The linear dependency of Envisat ASAR SWH error on collocation distance will be further investigated in Subsection 4.3.

Another feature which is apparent from the comparison between Figures 5 and 6, or between Tables 1 and 2, is the reduction of SWH error in deep and open ocean, regardless of Envisat ASAR,

NDBC buoy and ww3 wave model data, both in terms of RMSE and SI. A possible contributing factor of the larger error in the coastal regions may be the larger spatial variability of the ocean wave field in the coastal shallow waters. The further analysis and discussion on the reason for the smaller error of Envisat ASAR SWH in the deep ocean will be presented in the Subsection 4.4.

Table 1. Estimates of calibration coefficients, RMSE and SI for the triple collocated SWH datasets from all the 152 buoys, Envisat ASAR and ww3 model hindcasts.

Collocation	Calibration Coefficients		RMSE (m)			SI		
Distance (km)	β_{ASAR}	β_{ww3}	$RMSE_{buoy}$	$RMSE_{ASAR}$	$RMSE_{ww3}$	SI_{buoy}	SI_{ASAR}	SI_{ww3}
50	0.9495	0.9583	0.2427	0.5660	0.2330	11.93%	27.84%	11.82%
60	0.9478	0.9618	0.2599	0.5725	0.2254	12.75%	28.08%	11.37%
70	0.9510	0.9670	0.2698	0.5738	0.2254	13.33%	28.26%	11.39%
80	0.9558	0.9716	0.2864	0.5710	0.2148	14.18%	28.08%	10.83%
90	0.9583	0.9743	0.3027	0.5665	0.2042	15.08%	28.00%	10.33%
100	0.9604	0.9771	0.3068	0.5617	0.2039	15.37%	27.87%	10.34%
110	0.9619	0.9822	0.3191	0.5607	0.1953	16.08%	27.94%	9.92%
120	0.9649	0.9842	0.3295	0.5646	0.1925	16.59%	28.03%	9.74%
130	0.9642	0.9852	0.3366	0.5663	0.1897	16.90%	28.04%	9.56%
140	0.9629	0.9866	0.3415	0.5678	0.1921	17.03%	27.98%	9.61%
150	0.9631	0.9886	0.3466	0.5698	0.1938	17.23%	28.00%	9.65%
160	0.9622	0.9904	0.3522	0.5721	0.1969	17.43%	28.02%	9.74%
170	0.9609	0.9917	0.3557	0.5762	0.1986	17.55%	28.15%	9.79%
180	0.9592	0.9920	0.3575	0.5773	0.2012	17.60%	28.17%	9.88%
190	0.9581	0.9917	0.3605	0.5787	0.2017	17.71%	28.22%	9.89%
200	0.9583	0.9927	0.3643	0.5789	0.2021	17.90%	28.23%	9.90%

Table 2. As in Table 1, but for collocated datasets with the 54 buoys only in the deep and open ocean.

Collocation	Calibration Coefficients		RMSE (m)			SI		
Distance (km)	β_{ASAR}	β_{ww3}	$RMSE_{buoy}$	$RMSE_{ASAR}$	$RMSE_{ww3}$	SI_{buoy}	SI_{ASAR}	SI_{ww3}
50	0.9044	0.9614	0.2176	0.5017	0.1887	9.61%	23.62%	8.59%
60	0.8989	0.9622	0.2253	0.5131	0.1875	9.85%	24.02%	8.45%
70	0.9034	0.9637	0.2289	0.5122	0.1799	10.05%	23.97%	8.14%
80	0.9069	0.9650	0.2376	0.5108	0.1789	10.47%	23.92%	8.12%
90	0.9091	0.9661	0.2433	0.5094	0.1792	10.76%	23.95%	8.16%
100	0.9075	0.9663	0.2415	0.5095	0.1848	10.75%	24.14%	8.46%
110	0.9055	0.9662	0.2442	0.5072	0.1837	10.92%	24.20%	8.46%
120	0.9057	0.9669	0.2545	0.5167	0.1779	11.36%	24.57%	8.16%
130	0.9046	0.9666	0.2596	0.5188	0.1790	11.55%	24.61%	8.19%
140	0.9042	0.9687	0.2669	0.5227	0.1778	11.81%	24.67%	8.08%
150	0.9049	0.9699	0.2677	0.5236	0.1819	11.84%	24.69%	8.25%
160	0.9034	0.9712	0.2676	0.5284	0.1870	11.78%	24.82%	8.43%
170	0.9028	0.9716	0.2700	0.5330	0.1866	11.85%	24.99%	8.39%
180	0.9024	0.9722	0.2699	0.5343	0.1896	11.82%	25.01%	8.50%
190	0.9016	0.9719	0.2717	0.5363	0.1910	11.89%	25.09%	8.55%
200	0.9014	0.9723	0.2738	0.5383	0.1899	11.98%	25.10%	8.51%

Figure 5. Scatter plots of the comparison results with all the 152 buoys, for Envisat ASAR *vs.* NDBC buoys (**the left panels**), Envisat ASAR *vs.* ww3 model (**the middle panels**), and ww3 model *vs.* NDBC buoys (**the right panels**). The collocation distances between ASAR and buoy in the plots from upper to bottom panels are 50 km, 100 km, 150 km and 200 km, respectively. The numbers in the color bar represent the number of collocated data points per 0.1 m histogram bins.

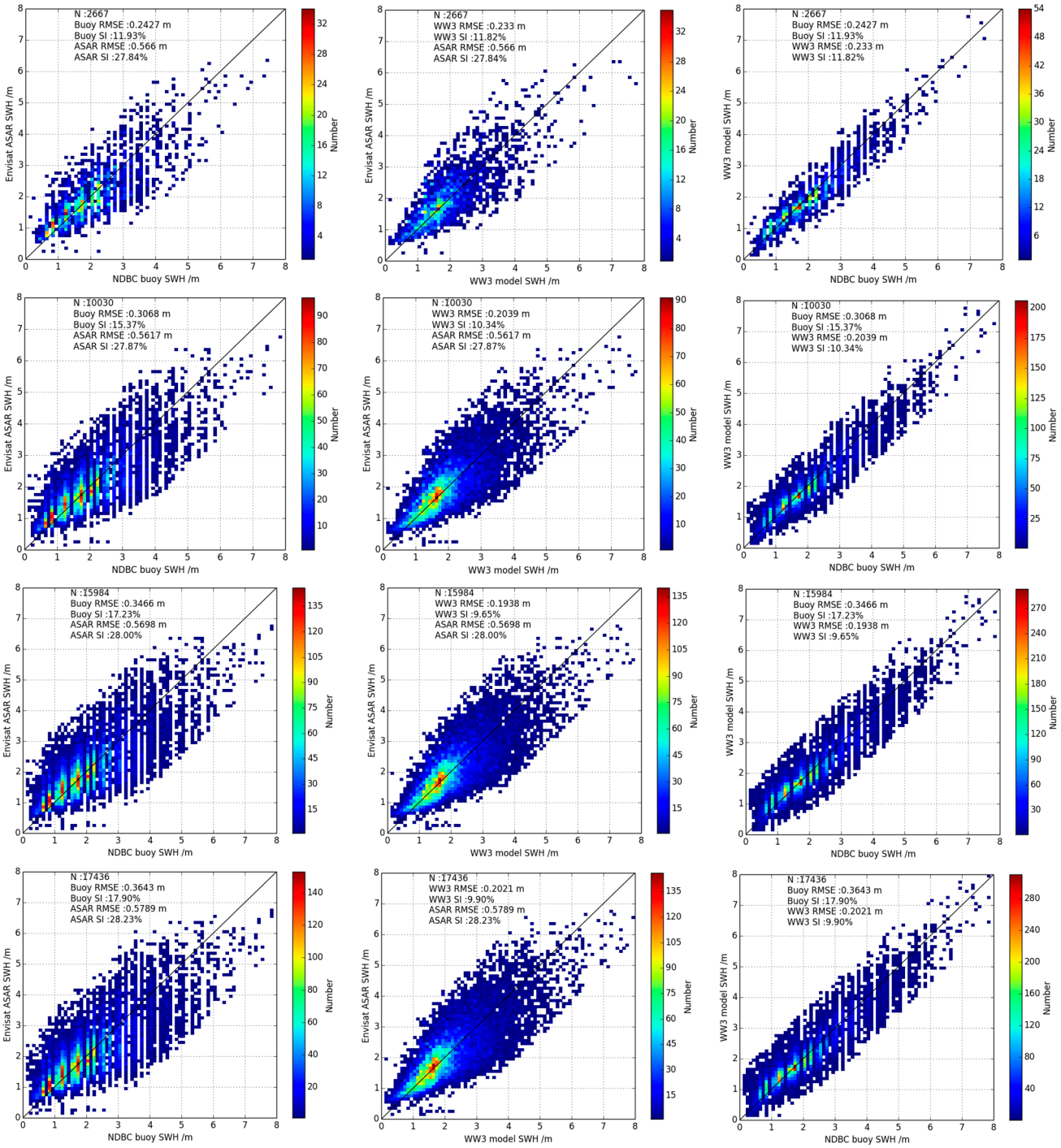

Figure 6. As in Figure 5, but for datasets with 54 buoys only in the deep and open ocean.

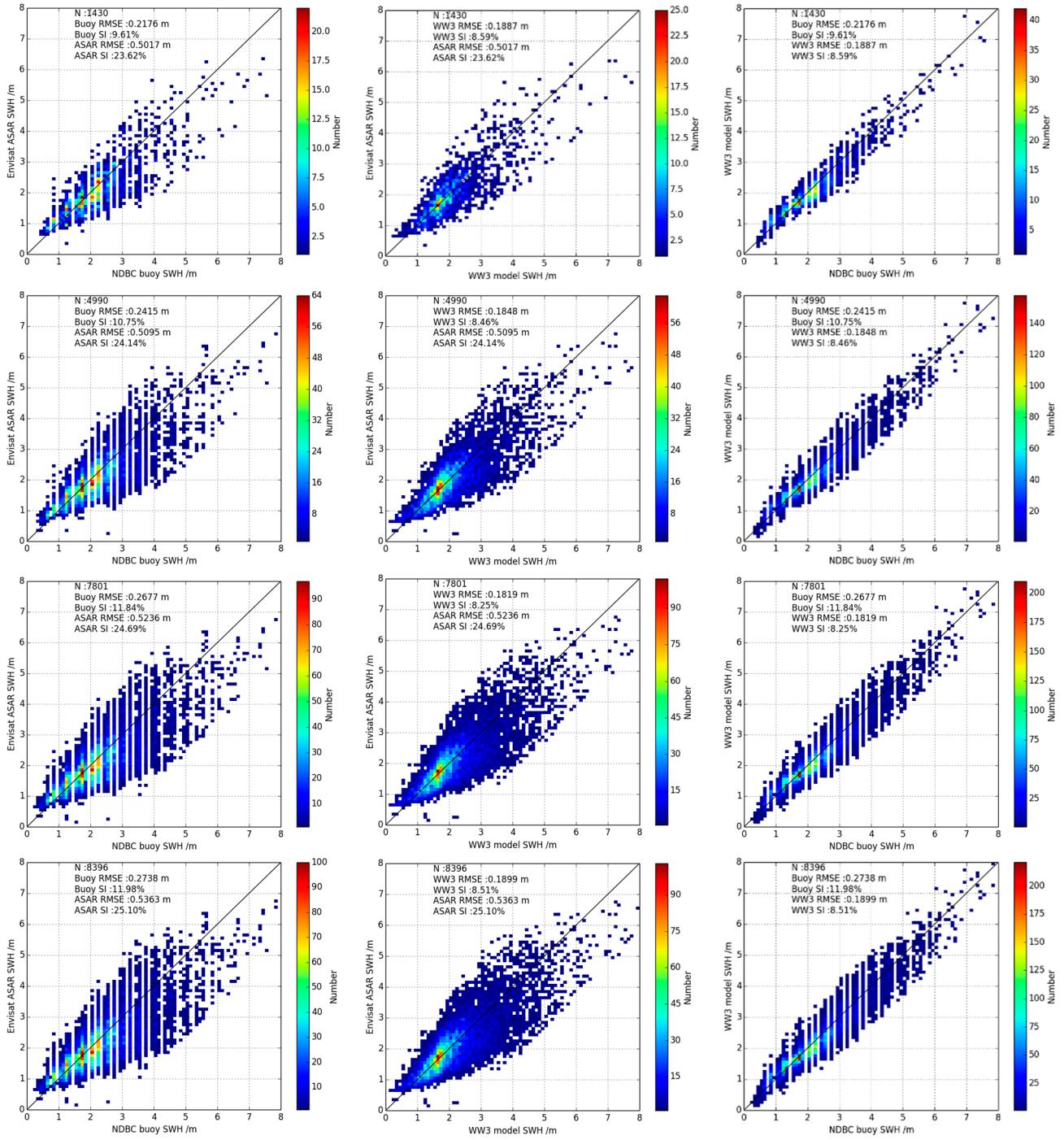

4.3. Error Analysis on Collocation Distance

The estimation of the error for the Envisat ASAR derived SWH with the dependence of the collocation distance is shown in Figure 7. In the figure, the circles and lines refer the RMSE of Envisat ASAR SWH and the regression lines, respectively, while the blue and red symbols indicate the results from all buoys and those deployed in the deep and open ocean. It is shown that, the errors of Envisat ASAR are linear to the collocation distance, and decrease with the decreasing collocation distance.

For RMSE of Envisat ASAR wave mode derived SWH estimated from datasets with all buoys and those in the deep and open ocean, linear regressions were performed with collocation distance. This

provides RMSE as a linear function of collocation distance D, given by Equations (6) and (7), for all buoys and the deep open ocean buoys collocations, respectively,

$$RMSE_{ASAR} = 0.1209 \times 10^{-3} D + 0.5551 \quad (6)$$

$$RMSE_{ASAR} = 0.2389 \times 10^{-3} D + 0.4899 \quad (7)$$

Using the linear function above, the error of Envisat ASAR for significant wave height with zero collocation distance can be obtained. Theoretically, with this collocation distance, the buoy and satellite measurements were collocated exactly in space, which could be hardly achieved using the direct comparison of ASAR products and buoy observations. The RMSEs of 0.5551 m and 0.4899 m for the Envisat ASAR SWH are found for the regions of all buoys and those deployed in the deep and open ocean, respectively.

Figure 7. Change of Envisat ASAR wave mode SWH errors as functions of the collocation distance. Circles and lines refer the RMSEs of ASAR SWH estimated from triple collocations and the regression lines, respectively. Blue and red symbols indicate the results from all buoys and deep-and-open-ocean buoys, respectively.

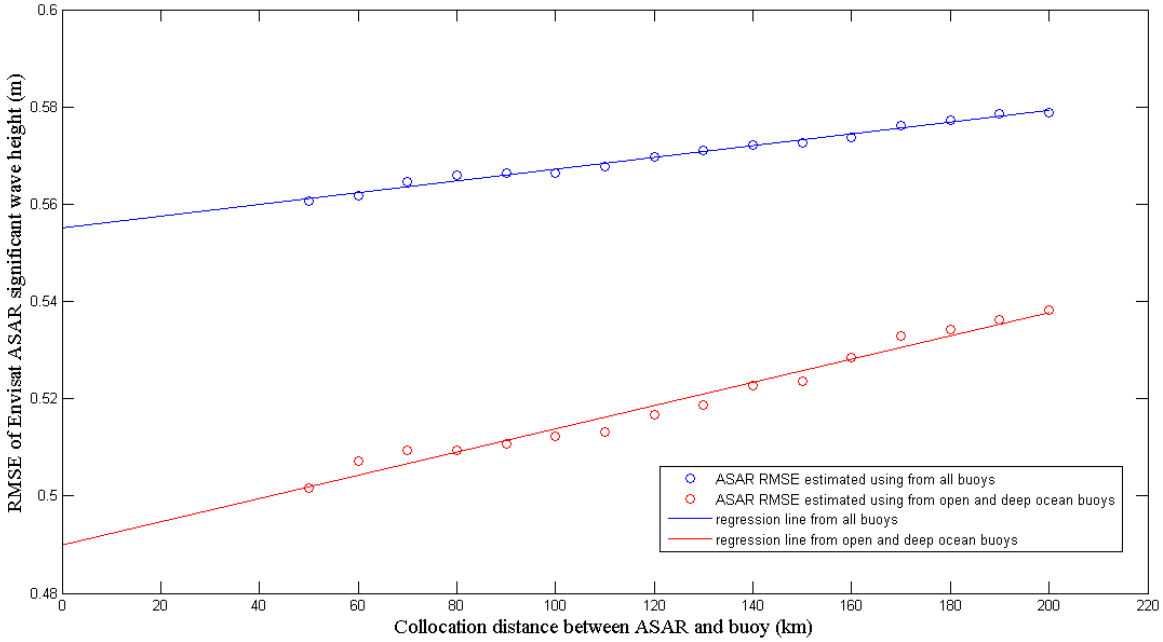

4.4. Discussion on Error of Envisat ASAR Wave Mode SWH in Coastal Waters

As pointed out above, the triple collocated comparison indicates that the SWH errors of Envisat ASAR wave mode data are smaller in the deep and open ocean than the coastal regions. One of the major reasons is that the performance of the ocean wave retrieval algorithm of Envisat ASAR wave mode may be poor in the coastal waters, due to the modulation transfer function (MTF).

The SAR MTF T adopted in the ASAR wave mode retrieval algorithm, consists of Real Aperture Radar (RAR) MTF T^R and velocity bunching MTF [1]:

$$T = -j\beta k_x T^v + T^R \quad (8)$$

$$T^v = -\omega\left(k_y / K\sin\theta + j\cos\theta\right) \tag{9}$$

where β represents the range to velocity ratio of the SAR platform, θ the radar incidence angle, T^v the orbital velocity transfer function and $j^2 = -1$. And K, k_y and k_y are wavenumber, and its components in azimuth and radar look direction, respectively.

In the Envisat ASAR wave mode retrieval algorithm, the angular frequency ocean wave ω is given as the deep-water dispersion relation [30]

$$\omega = \sqrt{gK} \tag{10}$$

regardless of the water depth the SAR imagette acquired. However, in finite depth water, the ocean wave dispersion relation should be

$$\omega^2 = gK\tanh\left(Kd\right) \tag{11}$$

with water depth d.

The inaccurate dispersion relation may bring error into SAR MTF, and finally the Envisat ASAR wave mode SWH retrievals. In [38], Collard *et al.* noticed this inaccuracy and applied the finite depth dispersion relation in their inversion scheme for Envisat ASAR image mode imagery. Moreover, as the successor of Envisat ASAR, the Sentinel-1A, which was launched on 3 April 2014, has fixed this inaccuracy in its retrieval algorithm for Ocean Swell Spectra component of the Level 2 Ocean product [39].

Therefore, the MTF adopted in the algorithm assuming that observed waves are in deep water should be responsible for the larger errors in some coastal regions.

4.5. Discussion on the Triple Collocation Results

In this paper, we have applied the triple collocation technique to assess the quality of the ESA's Envisat ASAR wave mode SWH product. Therefore, it is interesting to discuss this first validation result from triple collocation technique with the previous studies, both the triple collocated comparison for the altimeter SWH, and the conventional comparison for the Envisat ASAR SWH.

As shown in Section 4.2, the triple collocation analysis produced the result that the Envisat ASAR has the largest error, followed by buoy errors, and the ww3 wave model has the smallest. The performance of buoy data may cause a little surprise, because the buoy SWH measurements are generally assumed to be of high quality and be used in numerous validation studies as the "truth" data. In fact, this finding is consistent with the previous altimeter SWH triple collocated validation result. In the triple collocation analysis on SWH from ERS altimeter, ECMWF (European Centre for Medium-Range Weather Forecasts) wave model and buoys, the buoy errors were also found to be the largest [26]. In their work, Janssen *et al.* attributed the largest error of buoy SWH data to the representativeness error, and the quality control issues [26]. Although this could be a possible explanation of the larger buoy errors found here, it remains further studies.

Li *et al.* presented a validation and inter-comparison of ESA's SWH derived from Envisat ASAR wave mode against buoy and wave model, and an RMSE of 0.88 m and 0.65 m were found in the comparison in respect to buoy and wave model, respectively [19]. Both are larger than the triple collocation analysis result here (0.55 m derived from dataset containing all buoys). The reason why the error from conventional comparison are larger may be that the triple collocation technique here could

produce the "absolute" error, while conventional inter-comparison only yields the errors in respect to buoy or wave model and errors from the buoy and model data are not taken into consideration.

From the scatter plots in Figures 5 and 6, it is clear that the ASAR derived SWH has significant underestimation for high sea state, particularly when SWH is above 5 m, compared to the buoy or ww3 SWH. This saturation effect can be also found in previous validation studies [15,19], and it is due to the stronger azimuth cut-off effect in high wave cases, affecting the quasi-linear assumption in the Envisat ASAR wave mode retrieval algorithm. Thus, it should be pointed out that the result (*i.e.*, absolute error is less than 0.5 m in open ocean) revealed here could be not applied for the sea state above this threshold.

5. Conclusions

The triple collocation error model technique is a promising method to estimate the error structures from remote sensing retrievals. In this paper, the triple collocation error model is applied to the error estimation and analysis on Envisat ASAR wave mode derived SWH data for the first time, using NDBC buoy and ww3 wave model data.

Overall, SWH error of Envisat ASAR wave mode is in the order of 0.5 m and 24% for RMSE and SI, which much larger than that of NDBC buoy and ww3 wave model. The analysis on the Envisat ASAR SWH error trend of the collocation distance shows a linear dependency of error on distance. Utilizing this linear relation, the absolute error of Envisat ASAR wave height was obtained with zero collocation distance. The RMSEs of 0.56 m and 0.49 m for the Envisat ASAR wave mode SWH are presented for the regions of all buoys and buoys in the deep and open ocean, respectively.

The comparison results show that the errors of Envisat ASAR SWH are larger in the coastal waters. The explanations for that are inaccurate MTF of the retrieval algorithm and larger spatial variability of the ocean wave field in the coastal shallow waters.

Acknowledgments

The Envisat ASAR wave mode data has been provided from the Dragon-3 project (ID 10412) and copyrighted to ESA. We are also grateful for the free access to buoy measurements provided by NDBC. The work was partly supported by financial sponsorship of the China Scholarship Council (CSC) when He Wang was in Laboratoire d'Océanographie Spatiale, IFREMER as a visiting scholar. And the work was also supported by funding from the Open Fund of State Key Laboratory of Satellite Ocean Environment Dynamics, Second Institute of Oceanography, State Oceanic Administration of China (No. SOED1410).

Author Contributions

He Wang designed and implemented the triple colocation validation method for Envisat ASAR wave mode data. All authors contributed to the conception of the paper, data processing, analysis, discussion and manuscript writing.

List of All Acronyms

ASAR	Advanced Synthetic Aperture Radar
CDIP	Coastal Data Information Program

Envisat	Environmental Satellite
ECMWF	European Centre for Medium-Range Weather Forecasts
ERS	European Remote Sensing Satellite
IFREMER	Institut Français de Recherche pour l'Exploitation de la Mer
IOWAGA	Integrated Ocean Waves for Geophysical and other Applications
MEDS	Marine Environmental Data Service
MTF	Modulation Transfer Function
NDBC	National Data Buoy Centre
NOAA	National Oceanic and Atmospheric Administration
RAR	Real Aperture Radar
RMSE	Root Mean Square Error
SAR	Synthetic Aperture Radar
SI	Scatter Index
SWH	Significant Wave Height
ww3	WaveWatch III

Conflicts of Interest

The authors declare no conflict of interest.

References

1. Hasselmann, K.; Hasselmann, S. On the nonlinear mapping of an ocean wave spectrum into a synthetic aperture radar image spectrum and its inversion. *J. Geophys. Res.* **1991**, *96*, 10713–10729.
2. Krogstad, H.E.; Barstow, S.F. Satellite wave measurement for coastal engineering applications. *Coast. Eng.* **1999**, *37*, 283–307.
3. Hasselmann, K.; Chapron, B.; Aouf, L.; Ardhuin, F.; Collard, F.; Engen, G.; Hasselmann, S.; Heimbach, P; Janssen, P.A.E.M.; Johnsen, H.; *et al.* The ERS SAR wave mode: A breakthrough in global ocean wave observations. In *ERS Missions: 20 Years of Observing Earth*, 1st ed.; Fletcher, K., Ed.; European Space Agency: Noordwijk, The Netherlands, 2013; pp. 165–198.
4. Chapron, B.; Collard, F.; Johnsen, H.; Engen, G. ASAR Wave mode first geophysical results. In Proceedings of 2002 ENVISAT Calibration Review Meeting, ESTEC, Noordwijk, The Netherlands, 9–13 September 2002.
5. Li, X.M.; Lehner, S.; Bruns, T. Ocean wave integral parameter measurements using ENVISAT ASAR wave mode data. *IEEE Trans. Geosci. Remote Sens.* **2011**, *49*, 155–174.
6. Li, X.M.; Lehner, S.; Bruns, T. Simultaneous measurements of global ocean waves by ASAR and Radar Altimeter onboard ENVISAT. *IEEE Trans. Geosci. Remote Sens.* **2014**, *52*, 2508–2518.
7. Malenovsky, Z.; Rott, H.; Cihlar, J.; Schaepman, M.; Garcia-Santos, G.; Fernandes, R.; Berger, M. Sentinels for science: Potential of Sentinel-1, -2, and -3 missions for scientific observations of ocean, cryosphere, and land. *Remote Sens. Environ.* **2012**, *120*, 91–101.

8. Husson, R.; Mouche, A.; Collard, F.; Johnsen, H.; Grouazel, A.; Chapron, B.; Coat, M.; Vincent, P.; Hajduch, G. Sentinel-1 advanced capabilities for improved wave spectra estimation and beyond. In Proceedings of the 2014 Waves in Shallow Water Environment Meeting, Reading, UK, 8–12 June 2014.
9. Aouf, L.; Lefevre, J.M.; Hauser, D.; Chapron, B. On the combined assimilation of RA-2 and ASAR wave data for the improvement of wave forecasting. In Proceedings of the 2006 15 Years of Radar Altimetry Symposium, Venice, Italy, 13–18 March 2006.
10. Ardhuin, F.; Chapron, B.; Collard, F. Observation of swell dissipation across oceans. *Geophys. Res. Lett.* **2009**, *36*, doi:10.1029/2008GL037030.
11. De Farias, E.G.G.; Lorenzzetti, J.A.; Bentamy, A.; Chapron, B.; Husson, R. Fuzzy logic applied to track generation areas of swell systems observed by SAR. *IEEE Trans. Geosci. Remote Lett.* **2012**, *9*, 841–845.
12. Voorrips, A.G.; Mastenbroek, C.; Hansen, B. Validation of two algorithms to retrieve ocean wave spectra from ERS synthetic aperture radar. *J. Geophys. Res.* **2001**, *106*, 16825–16840.
13. Violante-Carvalho, N.; Robinson, I.S.; Schulz-Stellenfleth, J. Assessment of ERS synthetic aperture radar wave spectra retrieved from the Max-Planck-Institut (MPI) scheme through intercomparisons of 1 year of directional buoy measurements. *J. Geophys. Res.* **2005**, *110*, doi:10.1029/2004JC002382.
14. Collard, F.; Ardhuin, F.; Chapron, B. Monitoring and analysis of ocean swell fields from space: New methods for routine observations. *J. Geophys. Res.* **2009**, *114*, doi:10.1029/2008JC005215.
15. Wang, H.; Zhu, J.H.; Yang, J.S.; Shi, C.Y. A semiempirical algorithm for SAR wave height retrieval and its validation using Envisat ASAR wave mode data. *Acta Oceanol. Sin.* **2012**, *31*, 59–66.
16. Zhang, B.; Perrie, W.; He, Y.J. Remote sensing of ocean waves by along-track interferometric synthetic aperture radar. *J. Geophys. Res.* **2009**, *114*, doi:10.1029/2009JC005310.
17. Zhang, B.; Perrie, W.; He, Y.J. Validation of RADARSAT-2 fully polarimetric SAR measurements of ocean surface waves. *J. Geophys. Res.* **2010**, *115*, doi:10.1029/2009JC005887.
18. Heimback, P.; Hasselmann, S.; Hasselmann, K. Statistical analysis and intercomparison of WAM model data with global ERS-1 SAR wave mode spectral retrievals over 3 years. *J. Geophys. Res.* **1998**, *103*, 7931–7977.
19. Li, X.M.; KönigKonig, T.; Schulz-Stellenfleth, J.; Lehner, S. Validation and intercomparison of ocean wave spectra inversion schemes using ASAR wave mode data. *Int. J. Remote Sens.* **2010**, *31*, 4969–4993.
20. Krogstad, H.E.; Wolf, J.; Thompson, S.P.; Wyatt, L.R. Methods for intercomparison of wave measurements. *Coast. Eng.* **1999**, *37*, 235–257.
21. Stoffelen, A. Toward the true near-surface wind speed: Error modeling and calibration using triple collocation. *J. Geophys. Res.* **1998**, *103*, 7755–7766.
22. Portabella, M.; Stoffelen, A. On scatterometer ocean stress. *J. Atmos. Ocean. Technol.* **2009**, *26*, 368–382.
23. Vogelzang, J.; Stoffelen, A.; Verhoef, A.; Figa-SaldañaSaldana, J. On the quality of high-resolution scatterometer winds. *J. Geophys. Res.* **2011**, *116*, doi:10.1029/2010JC006640.
24. Chakraborty, A.; Kumar, R.; Stoffelen, A. Validation of ocean surface winds from the OCEANSAT-2 scatterometer using triple collocation. *Remote Sens. Lett.* **2013**, *4*, 85–94.

25. Caires, S.; Sterl, A. Validation of ocean wind and wave data using triple collocation. *J. Geophys. Res.* **2003**, *108*, doi:10.1029/2002JC001491.
26. Janssen, P.A.E.M.; Abdalla, S.; Hersbach, H.; Bidlot, J.R. Error estimates of buoy, satellite, and model wave height data. *J. Atmos. Ocean. Technol.* **2007**, *24*, 1665–1677.
27. Abdalla, S.; Janssen, P.A.E.M.; Bidlot, J.R. Altimeter near real time wind and wave products: Random error estimation. *Mar. Geod.* **2011**, *34*, 393–406.
28. Chen, G.; Lin, H. Impacts of collocation window on the accuracy of altimeter/buoy wind-speed comparison—A simulation study. *Int. J. Remote Sens.* **2001**, *22*, 35–44.
29. Chen, G.; Xu, P.; Fang C.Y. Numerical simulation on the choice of space and time windows for altimeter/buoy comparison of significant wave height. In Proceedings of the 2000 IEEE International Geoscience and Remote Sensing Symposium, Honolulu, HI, USA, 24–28 July 2000.
30. Engen, G.; Johnsen, H.; HøgdaHogda, K.A.; Chapron, B.; Collard, F. *Envisat ASAR Level 2 Wave Mode Product Algorithm Specification—Software Requirements Document (Version 2.2.9)*; ESA ESTEC Contract "Envisat ASAR Wind & Wave Measurements from Level 1 Product" Report; Norut IT: Tromsø, Norway, 2005.
31. Chapron, B.; Johnsen, H.; Garello, R. Wave and wind retrieval from SAR images of the ocean. *Ann. Telecommun.* **2001**, *56*, 682–699.
32. Engen, G.; Johnsen, H. SAR-ocean wave inversion using image cross spectra. *IEEE Trans. Geosci. Remote Sens.* **1995**, *33*, 1047–1056.
33. Ardhuin, F.; Hanafin, J.; Quilfen Y.; Chapron B.; Queffeulou P.; Obrebski M.; Sienkiewicz J.; Vandemark D. Calibration of the "IOWAGA" global wave hindcast (1991–2011) using ECMWF and CFSR wind. In Proceedings of the 2011 International Workshop on Wave Hindcasting and Forecasting and 3rd Coastal Hazard Symposium, Kona, HI, USA, 30 October–4 November 2011.
34. Rascle, N.; Ardhuin, F.; Queffeulou, P.; Croize-Fillon, D. A global wave parameter database for geophysical applications. Part 1: Wave-current-turbulence interaction parameters for the open ocean based on traditional parameterizations. *Ocean Model.* **2008**, *25*, 154–171.
35. Ardhuin, F.; Rogers, E.; Babanin, A.V.; Filipot, J.R.; Magne, R.; Roland, A.; Van der Westhuysen, A.J.; Queffeulou, P.; Lefevre, J.M.; Aouf, L.; *et al*. Semiempirical dissipation source functions for ocean waves. Part I: Definition, calibration, and validation. *J. Phys. Oceanogr.* **2010**, *40*, 1917–1941.
36. Marsden, R.F. A proposal for a neutral regression. *J. Atmos. Ocean. Technol.* **1999**, *16*, 876–883.
37. Zwieback, S.; Scipal, K.; Dorigo, W.; Wagner, W. Structural and statistical properties of the collocation technique for error characterization. *Nonlin. Process. Geophys.* **2012**, *19*, 69–80.
38. Collard, F.; Ardhuin, F.; Chapron, B. Extraction of coastal ocean wave fields from SAR images. *IEEE J. Ocean. Eng.* **2005**, *30*, 526–533.
39. Johnsen, H.; Collard, F. *Sentinel-1 Ocean Swell Wave Spectra (OSW) Algorithm Definition*; Sentinel-1 IPF Development (Project No.: 355) Report; Norut IT: Tromsø, Norway, 2010.